JACS
JOURNAL OF THE AMERICAN CHEMICAL SOCIETY

Communication

pubs.acs.org/JACS

Single-Crystal Structure of a Covalent Organic Framework

Yue-Biao Zhang,[†,§] Jie Su,[‡,§] Hiroyasu Furukawa,[†] Yifeng Yun,[‡] Felipe Gándara,[†] Adam Duong,[†] Xiaodong Zou,*[,‡] and Omar M. Yaghi*[,†]

[†]Department of Chemistry, University of California, and Materials Sciences Division, Lawrence Berkeley National Laboratory, Berkeley, California 94720, United States

[‡]Inorganic and Structural Chemistry and Berzelii Center EXSELENT on Porous Materials, Department of Materials and Environmental Chemistry, Stockholm University, Stockholm SE−106 91, Sweden

Supporting Information

ABSTRACT: The crystal structure of a new covalent organic framework, termed COF-320, is determined by single-crystal 3D electron diffraction using the rotation electron diffraction (RED) method for data collection. The COF crystals are prepared by an imine condensation of tetra-(4-anilyl)methane and 4,4′-biphenyldialdehyde in 1,4-dioxane at 120 °C to produce a highly porous 9-fold interwoven diamond net. COF-320 exhibits permanent porosity with a Langmuir surface area of 2400 m^2/g and a methane total uptake of 15.0 wt % (176 cm^3/cm^3) at 25 °C and 80 bar. The successful determination of the structure of COF-320 directly from single-crystal samples is an important advance in the development of COF chemistry.

The linking of organic building units through strong bonds typically yields poorly crystalline or amorphous solids, thus precluding the characterization of their structures at the atomic level. Recent progress in this area has led to microcrystalline materials of covalent organic frameworks (COFs) based entirely on strong covalent linkages (B−O, C−N, and B−N) between building units.[1−7] The crystal structures of these COFs have traditionally been determined by analysis of powder X-ray diffraction data and aided by consideration of geometry principles developed in reticular chemistry.[8] Therefore, without analyzing single-crystal samples of COFs, uncertainties still remain regarding their precise atomic structure. Although a single crystalline form of a covalent organic network was recently reported, the building units making up the structure are held together by significantly weaker linkages (*trans* azodioxy, 20−30 kcal/mol) than those typically used to make COFs (e.g., imine linkages, >100 kcal/mol).[9] These weak linkages greatly facilitate crystallization but unfortunately lead to frail architectures with no permanent porosity.[9]

Here, we report the single-crystal structure of a new COF determined by 3D rotation electron diffraction (RED)[10]—a technique applied in this context for the first time. Electron diffraction (ED) is a useful technique for the structure determination of micro- and nanosized single crystals.[11,12] Crystals of this COF were prepared by the condensation of tetra-(4-anilyl)methane (as shown in Scheme 1: the tetrahedral unit, **A**) and 4,4′-biphenyldialdehyde (the linear ditopic linker, **B**) to form the corresponding COF termed COF-320 (**C**) having an imine-linked three-dimensional extended structure based on the diamond topology.

Scheme 1. Synthesis of COF-320 and Its Molecular Analogue

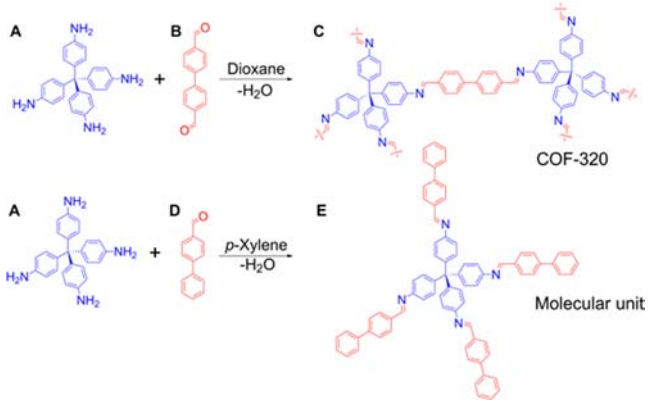

A mixture of **A** (100 mg, 0.263 mmol) and **B** (100 mg, 0.476 mmol) in 1,4-dioxane (5 mL) and aqueous acetic acid (3 mol/L, 1 mL) was sealed in a Pyrex tube and heated at 120 °C for 3 days. The resulting yellow precipitate was collected by filtration and washed with anhydrous 1,4-dioxane and tetrahydrofuran (THF), and it was subsequently activated using the supercritical CO_2 drying protocol[13] yielding a guest-free sample of 120 mg (70% based on **B**). The chemical formula of the activated COF-320 was determined from the elemental analysis (Calcd for $C_{53}H_{36}N_4$: C, 87.33; H, 4.98; N, 7.69%. Found: C, 86.99; H, 4.91; N, 7.51%). A molecular analogue **E** was synthesized and used for comparison in the analyses of the FT-IR and solid-state NMR spectra of COF-320. The FT-IR spectrum of an activated sample of COF-320 shows characteristic imine stretching vibrations at 1620 and 1200 cm^{-1} (1626 and 1202 cm^{-1} for **E**; see Figures S2−S6) corresponding to C═N and C−C═N−C stretching vibrations, respectively.[3a] The ^{13}C cross-polarization with magic-angle spinning (CP/MAS) solid-state NMR spectrum of COF-320 shows a chemical shift for the imine-^{13}C at 158.4 ppm (160.9 ppm for **E**), which is distinct from the aldehyde-^{13}C of starting material **B** at 193.6 ppm (see Figures S7−S10).[3a] The ^{15}N CP/MAS and high-power

Received: August 31, 2013
Published: October 21, 2013

dx.doi.org/10.1021/ja409033p | J. Am. Chem. Soc. 2013, 135, 16336−16339

decoupling MAS solid-state NMR spectra were acquired with a ^{15}N-isotope labeled sample of COF-320, which both show the imine-^{15}N chemical shift at 324 ppm and the residual aniline-^{15}N at 53 ppm (see Figures S11–S12). These observations support the formation of the covalently linked extended solid.

Scanning electron microscopy (SEM) imaging of the as-synthesized sample of COF-320 shows only a homogeneous morphology, consisting of the aggregation of rice-shaped crystals with a minimal dimension of about 200 nm (Figure 1a). By ultrasonic oscillation of the sample in THF, single crystals of COF-320 were dispersed on a copper sample grid for transmission electron microscopy (TEM) study. 3D RED data of the COF-320 single crystals were collected on a JEOL JEM2100 TEM by combing small beam tilt and large goniometer tilt steps using the RED–data collection software.[14]

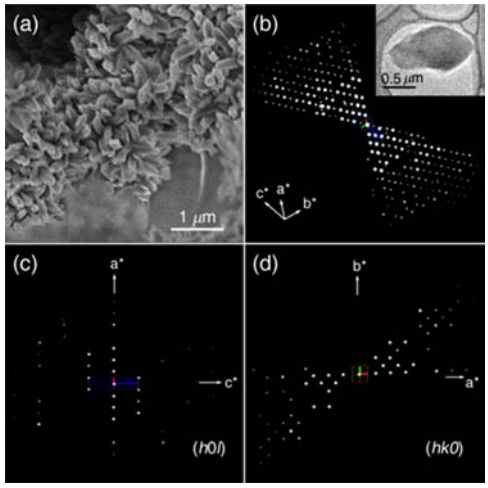

Figure 1. Morphology and electron diffraction of COF-320. (a) SEM image of the aggregation of crystallites. (b) The 3D reciprocal lattice of COF-320 reconstructed from the RED data collected from a crystal of 1.0 × 0.5 × 0.2 μm^3 (insert). (c) (*h*0*l*) and (d) (*hk*0) slices cut from the reconstructed reciprocal lattice.

RED data sets were collected at both 298 and 89 K. We found that COF-320 was electron beam sensitive and lowering the temperature reduced the beam damage. The RED data set collected at 89 K has a tilt range from −34.19° to 38.33° and a step width of 0.20°. In total, 396 ED frames were collected over 21 min. The 3D reciprocal lattice of COF-320 (Figure 1b–d) was reconstructed from the ED frames using the RED–data processing software.[14] 570 unique reflections with resolution up to 1.5 Å were obtained. The unit cell was determined from the 3D reciprocal lattice suggesting a body-centered tetragonal unit cell (a = 30.17 Å, c = 7.28 Å, V = 6628 Å^3). The reflection conditions obtained from the RED data suggest the space group to possibly be $I4_1md$ (No. 109) or $I\bar{4}2d$ (No. 122). The simulated annealing parallel tempering algorithm found in the FOX software package[15] was used to find a starting molecular arrangement from the 3D RED data. Finally, the crystal structure of COF-320 was solved in the space group $I\bar{4}2d$ and refined using the SHELXL software package.[16] All carbon and nitrogen atoms were refined isotropically, with soft restraints for the C–C and C═N bond lengths and the geometry of the phenyl ring being applied. All hydrogen atoms on the framework were added on the riding model, and the thermal displacement parameters were fixed for all of the non-hydrogen atoms. The agreement, R_1, value of the refinement converged to 0.31 after using the PLATON/SQUEEZE procedure[17] to deduct the contribution of diffraction from the highly disordered guest molecules in the pores (see Tables S3–S4).

The single-crystal structure of COF-320 exhibits a 3D extended framework by linking the tetrahedral organic building blocks and biphenyl linkers through imine bonds forming a diamond net. The resulting adamantane-like cage (Figure 2a; the cage dimensions from center-to-center distances between the tetrahedral carbon atoms is 30 × 30 × 65 Å^3) is elongated along the *c*-axis, which allows for a 9-fold interpenetration in this direction (Figure 2b). The overall structure has 1D rectangular channels with an aperture size of 13.5 Å × 6.2 Å running along the *c*-axis (Figure 2c). Although the structure is highly interpenetrated, COF-320 still possesses 49% of void volume.

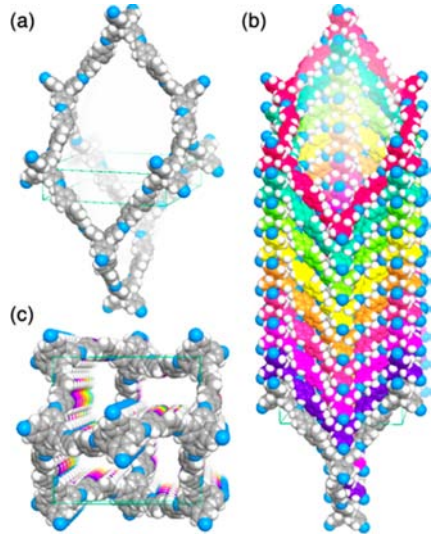

Figure 2. Single-crystal structure of COF-320 determined from RED data at 89 K. (a) Representative adamantane-like cage in the diamond net. (b) Structure of COF-320 viewed along the *a*-axis shows a 9-fold interpenetration of a diamond net. (c) The 1D rectangle-shaped channels along the *c*-axis.

The RED data set collected at 298 K suggests a body-centered orthorhombic unit cell (a = 27.93 Å, b = 31.31 Å, c = 7.89 Å, V = 6899 Å^3) and space group *Imma* (No. 74). With this data set we could only locate the central carbon atom of the tetrahedral building blocks, probably due to the relative low resolution of the RED data and from beam damage, which is more pronounced at higher temperatures. Nevertheless, based on the unit cell, space group, and atom coordinates determined from RED data, we were able to build a crystal structure model (Figure 3 and Table S5) using the Materials Studio 5.0 software package.[18]

The crystal structure of COF-320 at 298 K has the same connectivity and degree of interpenetration as the one at 89 K. The structural difference comes from the positional relation between the two nitrogen atoms on the biphenylbisimine fractions (the distance between them changed from 11.3 to 11.9 Å). The dimensions of the adamantane-like cage is now 28 × 31 × 71 Å^3. The distortion of the framework gives the crystal structure a lower symmetry and alters the 1D channel into a square shape with an aperture size of 11.5 Å × 11.5 Å (Figure 3c).

dx.doi.org/10.1021/ja409033p | J. Am. Chem. Soc. 2013, 135, 16336–16339

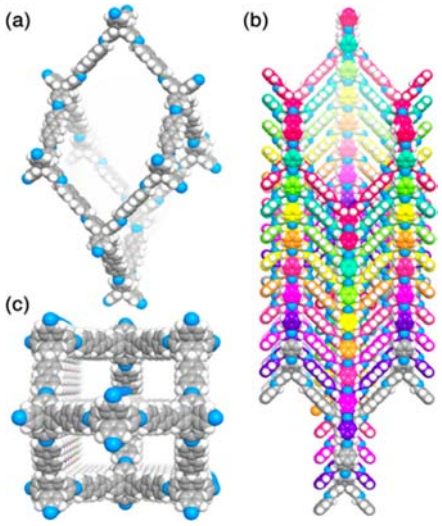

Figure 3. The crystal structure model of COF-320 based on the RED data at 298 K. (a) The adamantane-like cage in the diamond net. (b) The 9-fold interpenetration of the diamond net, viewed along the *a*-axis. (c) The 1D square-shaped channels running along the *c*-axis.

The PXRD pattern of the activated sample of COF-320 is in agreement with the calculated pattern from the model at 298 K (Figure 4; unit cell after refinement: a = 27.92(1) Å, b = 31.306(1) Å, c = 7.891(3) Å, V = 6897 (4) Å^3). In this case, the degree of interpenetration and the framework distortion observed in COF-320 preclude a structure solution based only on PXRD data and computer modeling, making the use of single-crystal diffraction data necessary for an accurate structure solution.

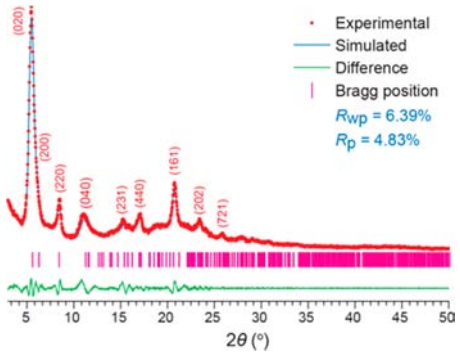

Figure 4. Indexed PXRD pattern of the activated sample of COF-320 (red) and the Pawley fitting (blue) from the modeled structure.

The presence of permanent porosity for an activated sample of COF-320 was confirmed by an Ar adsorption isotherm measurement at 87 K (Figure 5a). The profile of the isotherm is reminiscent of Ar and N_2 isotherms for COF-300;[3a] a steep Ar uptake was observed in the low relative pressure region (P/P_0 < 0.01), followed by a gradual increase of the uptake, ranging from P/P_0 = 0.1 to 0.35. Considering that the pore diameter of COF-320 from the crystal structure is in the micropore region, a unique profile of the isotherm accompanying a significant hysteresis loop is attributable to a guest-induced structural transformation and/or reorientation of the guest packing under increased pressure.[19] Due to the presence of steps, an accurate BET surface area estimation from the adsorption branch is not applicable. A pore volume of 0.81 cm^3/g can be estimated

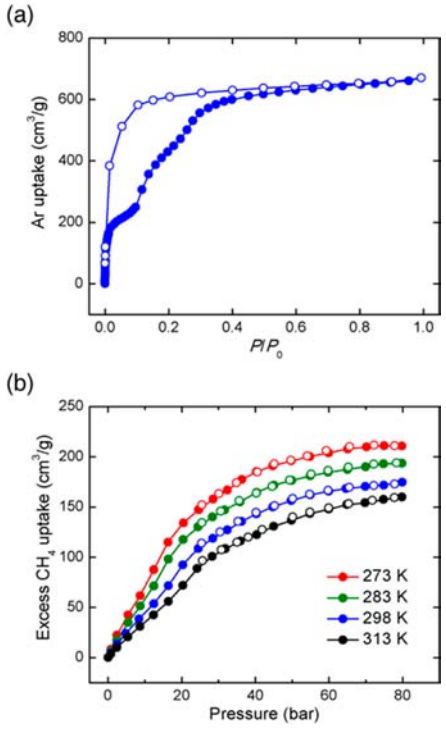

Figure 5. Gas adsorption measurements of COF-320: (a) Ar adsorption isotherm of COF-320 at 87 K. (b) High-pressure excess methane uptake at 273, 283, 298, and 313 K, respectively. Solid and open circles represent adsorption and desorption branches, respectively.

based on the DR plot method, which is equivalent to a Langmuir surface area of 2400 m^2/g. This result illustrates that even a high degree of interpenetration does not necessarily impede permanent porosity, which is in sharp contrast to previously reported crystalline materials in a 9-fold interpenetrated diamond net.[20]

COF-320 has relatively small pore diameter without sacrificing pore volume, making this COF material potentially suitable for room temperature methane storage. Therefore methane isotherms of COF-320 were measured up to 80 bar at 273, 283, 298, and 313 K (Figure 5b). These isotherms are nearly saturated at 80 bar, where excess methane uptake is 175 cm^3/g (= 11.1 wt %) at 80 bar and 298 K. We estimated total methane uptake using the pore volume of COF-320 and bulk density of methane (N_{total} = N_{excess} + (methane density) × (pore volume)), since total uptake cannot be measured experimentally.[21] Total methane uptake capacity is estimated to be 15.0 wt % at 80 bar and 298 K, which outperforms most of the 2D COFs.[21] This value is smaller than that for COF-102 (25 wt %) having a high BET surface area; however, volumetric total methane uptake for COF-320 is approaching that for COF-102 (176 and 203 cm^3/cm^3 for COF-320 and COF-102, respectively).[21]

In conclusion, we have determined the single-crystal structure of a highly porous new COF by collecting the 3D electron diffraction data with the RED method, which is a powerful tool for addressing the structure determination challenges encountered during the discovery of new COF materials.

dx.doi.org/10.1021/ja409033p | J. Am. Chem. Soc. 2013, 135, 16336−16339

■ ASSOCIATED CONTENT

Supporting Information

Detailed synthetic procedures and characterization, FT-IR and solid-state NMR spectra, SEM images, RED data collection, a movie showing the collected ED frames, structure determination and atomic coordinates from RED data, structure modeling and PXRD pattern analyses, TGA trace, low-pressure methane adsorption analysis, high-pressure methane isotherms, and crystallographic data (CIFs) are included. This material is available free of charge via the Internet at http://pubs.acs.org.

■ AUTHOR INFORMATION

Corresponding Authors

xzou@mmk.su.se
yaghi@berkeley.edu

Author Contributions

[§]These authors contributed equally.

Notes

The authors declare no competing financial interest.

■ ACKNOWLEDGMENTS

The work at Berkeley was partially supported for the synthesis by BASF SE (Ludwigshafen, Germany), general adsorption characterization by the U.S. Department of Energy (DOE) (DE-FG36-08GO18141), and methane adsorption by DOE ARPA-E (DE-AR0000251). The TEM work is supported by the Swedish Research Council (VR), the Swedish Governmental Agency for Innovation Systems (VINNOVA), and the Knut & Alice Wallenberg Foundation through a grant for purchasing the TEM and the project grant 3DEM-NATUR. J.S. was supported by a postdoctoral grant from the Wenner−Gren Foundation. We thank Dr. C. Canlas and Dr. X. Kong (UCB) for the acquisition of the solid-state NMR spectra, Mr. P. Klonowski (UCB/LBNL) for their valuable comments, and Mr. M. Veenstra (Ford Motor Company) for DOE ARPA-E project management.

■ REFERENCES

(1) (a) Côté, A. P.; Benin, A. I.; Ockwig, N. W.; O'Keeffe, M.; Matzger, A. J.; Yaghi, O. M. *Science* **2005**, *310*, 1166. (b) Tilford, R. W.; Gemmill, W. R.; zur Loye, H.-C.; Lavigne, J. J. *Chem. Mater.* **2006**, *18*, 5296. (c) El-Kaderi, H. M.; Hunt, J. R.; Mendoza-Cortés, J. L.; Côté, A. P.; Taylor, R. E.; O'Keeffe, M.; Yaghi, O. M. *Science* **2007**, *316*, 268. (d) Spitler, E. L.; Dichtel, W. R. *Nat. Chem.* **2010**, *2*, 672. (e) Bertrand, G. H. V.; Michaelis, V. K.; Ong, T. C.; Griffin, R. G.; Dincă, M. *Proc. Natl. Acad. Sci. U.S.A.* **2013**, *110*, 4923. (f) Hunt, J. R.; Doonan, C. J.; LeVangie, J. D.; Côté, A. P.; Yaghi, O. M. *J. Am. Chem. Soc.* **2008**, *130*, 11872.

(2) (a) Kuhn, P.; Antonietti, M.; Thomas, A. *Angew. Chem., Int. Ed.* **2008**, *47*, 3450. (b) Campbell, N. L.; Clowes, R.; Ritchie, L. K.; Cooper, A. I. *Chem. Mater.* **2009**, *21*, 204.

(3) (a) Uribe-Romo, F. J.; Hunt, J. R.; Furukawa, H.; Klöck, C.; O'Keeffe, M.; Yaghi, O. M. *J. Am. Chem. Soc.* **2009**, *131*, 4570. (b) Ding, S.-Y.; Gao, J.; Wang, Q.; Zhang, Y.; Song, W.-G.; Su, C.-Y.; Wang, W. *J. Am. Chem. Soc.* **2011**, *133*, 19816.

(4) Uribe-Romo, F. J.; Doonan, C. J.; Furukawa, H.; Oisaki, K.; Yaghi, O. M. *J. Am. Chem. Soc.* **2011**, *133*, 11478.

(5) Zhao, H. Y.; Jin, Z.; Su, H. M.; Jing, X. F.; Sun, F. X.; Zhu, G. S. *Chem. Commun.* **2011**, *47*, 6389.

(6) Nagai, A.; Chen, X.; Feng, X.; Ding, X. S.; Guo, Z. Q.; Jiang, D. L. *Angew. Chem., Int. Ed.* **2013**, *52*, 3770.

(7) Jackson, K. T.; Reich, T. E.; El-Kaderi, H. M. *Chem. Commun.* **2012**, *48*, 8823.

(8) O'Keeffe, M.; Peskov, M. A.; Ramsden, S. J.; Yaghi, O. M. *Acc. Chem. Res.* **2008**, *41*, 1782.

(9) Beaudoin, D.; Maris, T.; Wuest, J. D. *Nat. Chem.* **2013**, *5*, 830.

(10) Zhang, D.; Oleynikov, P.; Hovmöller, S.; Zou, X. *Z. Kristallogr.* **2010**, *225*, 94.

(11) (a) Zou, X.; Hovmöller, S. *Acta Crystallgr. A* **2008**, *64*, 149. (b) Martínez-Franco, R.; Moliner, M.; Yun, Y.; Sun, J.; Wan, W.; Zou, X.; Corma, A. *Proc. Natl. Acad. Sci. U.S.A.* **2013**, *110*, 3749.

(12) (a) Kolb, U.; Gorelik, T.; Kübel, C.; Otten, M. T.; Hubert, D. *Ultramicroscopy* **2007**, *107*, 507. (b) Feyand, M.; Mugnaioli, E.; Vermoortele, F.; Bueken, B.; Dieterich, J. M.; Reimer, T.; Kolb, U.; de Vos, D.; Stock, N. *Angew. Chem., Int. Ed.* **2012**, *51*, 10373.

(13) (a) Li, K. H.; Olsan, D. H.; Lee, J. Y.; Bi, W. H.; Wu, K.; Yuen, T.; Xu, Q.; Li, J. *Adv. Funct. Mater.* **2008**, *18*, 2205. (b) Furukawa, H.; Ko, N.; Go, Y. B.; Aratani, N.; Choi, S. B.; Choi, E.; Yazaydin, A. O.; Snurr, R. Q.; O'Keeffe, M.; Kim, J.; Yaghi, O. M. *Science* **2010**, *329*, 424.

(14) Wan, W.; Sun, J. L.; Su, J.; Hovmöller, S.; Zou, X. *J. Appl. Crystallogr.* **2013**, accepted.

(15) Favre-Nicolin, V.; Černý, R. *J. Appl. Crystallogr.* **2002**, *35*, 734.

(16) Sheldrick, G. *Acta Crystallgr. A* **2008**, *64*, 112.

(17) Spek, A. *Acta Crystallgr. D* **2009**, *65*, 148.

(18) Accelrys Software Inc. *Materials Studio 5.0: Modeling Simulation for Chemical and Material*, San Diego, CA, 2009.

(19) (a) Bureekaew, S.; Sato, H.; Matsuda, R.; Kubota, Y.; Hirose, R.; Kim, J.; Kato, K.; Takata, M.; Kitagawa, S. *Angew. Chem., Int. Ed.* **2010**, *49*, 7660. (b) Reichenbach, C.; Kalies, G.; Lincke, J.; Lassig, D.; Krautscheid, H.; Moellmer, J.; Thommes, M. *Microporous Mesoporous Mater.* **2011**, *142*, 592.

(20) (a) Hirsch, K. A.; Venkataraman, D.; Wilson, S. R.; Moore, J. S.; Lee, S. *Chem. Commun.* **1995**, 2199. (b) Hirsch, K. A.; Wilson, S. R.; Moore, J. S. *Chem.—Eur. J.* **1997**, *3*, 765. (c) Zhang, H.-X.; Yao, Q.-X.; Jin, X.-H.; Ju, Z.-F.; Zhang, J. *CrystEngComm* **2009**, *11*, 1807. (d) Cheng, J.-J.; Chang, Y.-T.; Wu, C.-J.; Hsu, Y.-F.; Lin, C.-H.; Proserpio, D. M.; Chen, J.-D. *CrystEngComm* **2012**, *14*, 537.

(21) Furukawa, H.; Yaghi, O. M. *J. Am. Chem. Soc.* **2009**, *131*, 8875.